nature chemistry

ARTICLES

PUBLISHED ONLINE: 1 JUNE 2015 | DOI: 10.1038/NCHEM.2270

An electrochemical clamp assay for direct, rapid analysis of circulating nucleic acids in serum

Jagotamoy Das[1], Ivaylo Ivanov[1], Laura Montermini[2], Janusz Rak[2], Edward H. Sargent[3] and Shana O. Kelley[1,4]*

The analysis of cell-free nucleic acids (cfNAs), which are present at significant levels in the blood of cancer patients, can reveal the mutational spectrum of a tumour without the need for invasive sampling of the tissue. However, this requires differentiation between the nucleic acids that originate from healthy cells and the mutated sequences shed by tumour cells. Here we report an electrochemical clamp assay that directly detects mutated sequences in patient serum. This is the first successful detection of cfNAs without the need for enzymatic amplification, a step that normally requires extensive sample processing and is prone to interference. The new chip-based assay reads out the presence of mutations within 15 minutes using a collection of oligonucleotides that sequester closely related sequences in solution, and thus allow only the mutated sequence to bind to a chip-based sensor. We demonstrate excellent levels of sensitivity and specificity and show that the clamp assay accurately detects mutated sequences in a collection of samples taken from lung cancer and melanoma patients.

The discovery that cell-free nucleic acids (cfNAs) released from tumours are present in the blood of patients with cancer has focused attention on their potential as a new marker for cancer diagnosis and management[1–3]. Detection of cfNAs in plasma or serum could serve as a liquid biopsy, potentially replacing tumour-tissue biopsies in certain diagnostic applications. Although cancer patients often have higher levels of cfNAs than do healthy controls, the levels of overall cfNAs vary considerably in plasma or serum samples in each group[4]. For the analysis of cfNAs to be clinically meaningful it must enable the specific detection of cancer-related sequences.

The detection of mutated sequences (for example, *KRAS* and *BRAF*) linked to cancer in cfNAs could allow the specific monitoring of tumour-related sequences[5,6]; however, this would require a very sensitive and specific approach to detect successfully low amounts of mutant genes in the presence of high levels of wild-type sequences in patient samples[7]. The existing approaches able to monitor cfNAs rely on the polymerase chain reaction (PCR)[8] or DNA sequencing[9]. DNA sequencing is an excellent approach for research studies that seek to profile large regions of DNA, but its implementation is prohibitively expensive for routine clinical use, and the slow turnaround time (2–3 weeks) is not ideal for optimal treatment outcomes[5]. PCR is not typically effective for the detection of point mutations, but the introduction of peptide nucleic acid (PNA) clamps boosts the accuracy of this approach[10–12]. The PNAs serve as sequence-selective clamps that prevent the amplification of wild-type DNA during PCR, and the mutated sequence is then amplified selectively. Unfortunately, as PCR is prone to interference from the components of biological samples, clamp PCR is not able to detect directly the cfNA mutations in blood or serum samples. Also, it can introduce bias based on the amplification efficiency of different sequences[4], and requires pre-processing of the samples and purification of the nucleic acids from large-volume samples (for example >5 ml)[13]. A method that is more accurate, and able to detect cfNA mutations directly in serum or blood, is thus required urgently.

Chip-based methods that leverage electronic or electrochemical readouts represent attractive alternatives for the analysis of clinical samples because they are amenable to automation and the development of cost-effective testing devices[14]. Electrochemical methods, in particular, have received significant attention because of their low cost and potential for high levels of multiplexing and sensitivity[15]. This type of testing approach has been applied successfully to the analysis of a subset of cancer biomarkers[16–20], as well as a variety of infectious pathogens[21–24], but the feasibility of analysing cfNAs for cancer-related mutations in clinical samples has not been established. Previous efforts to achieve point-mutation detection based on electrochemical methods[25,26] relied on the stringent control of assay conditions or mismatch-sensitive enzymes[27], but these types of approaches would not yield significant selectivity in heterogeneous patient samples in which a mutated sequence may be outnumbered by a high level of the wild-type sequence.

Here we report an electrochemical approach that is the first to enable the direct analysis of cfNAs from patient serum samples. Electrochemical sensors are functionalized with molecules that render them specific for the nucleic acid sequence of interest, and a series of clamp molecules is used to eliminate cross-reactivity with wild-type nucleic acids and with deliberately selected mutants. Electrochemical analysis has been used previously with a variety of clinically relevant analytes[28–32], but this is the first study that demonstrates the specific detection of cancer-related mutations in cfNAs. We show that the approach is highly specific, rapid and sensitive, reading sequences of interest in 5 fg of isolated RNA. We further show that it can be used with unprocessed banked serum from cancer patients and produces results that are consistent with the gold-standard method. The approach reported enables a much broader analysis of cfNAs in patient samples.

[1]Department of Pharmaceutical Sciences, Leslie Dan Faculty of Pharmacy, University of Toronto, Toronto M5S 3M2, Canada. [2]The Research Institute of the McGill University Health Centre, Montreal Children's Hospital, 1001 Decarie Blvd, Montreal, Quebec H4A 3J1, Canada. [3]Department of Electrical and Computer Engineering, Faculty of Engineering, University of Toronto, Toronto, Canada. [4]Department of Biochemistry, Faculty of Medicine, University of Toronto, Toronto, Ontario M5S 3M2, Canada. *e-mail: shana.kelley@utoronto.ca

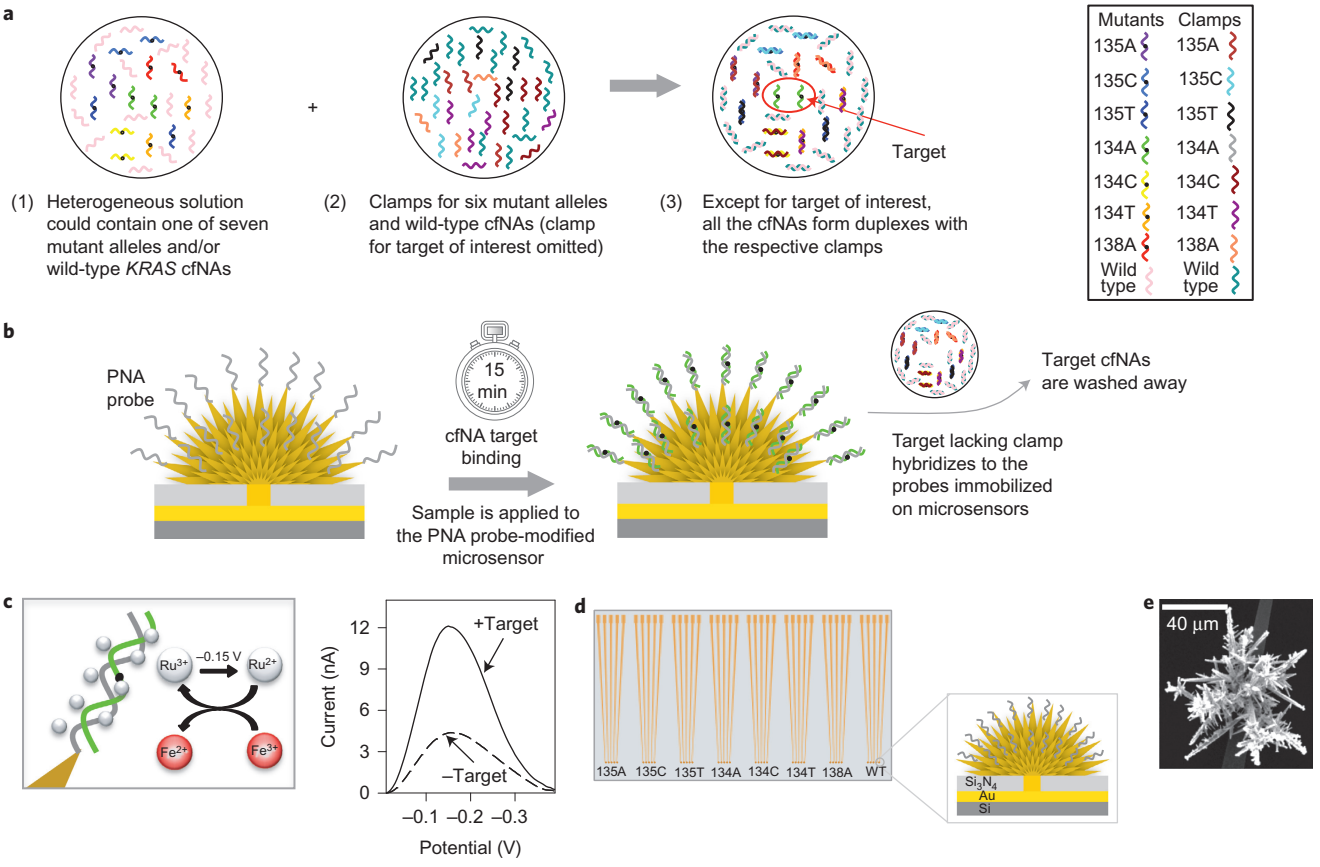

Figure 1 | The clamp chip for the electrochemical analysis of mutated cfNAs. a, Clamp strategy. Schematic representation of the clamp approach to detecting mutations of *KRAS*. The sample (1) is mixed with clamp sequences (2) that will sequester the wild-type sequence and all the mutants except the detection target. All the mutants and the wild-type sequence hybridize to the respective complementary clamps in solution (3), except the target of interest, for example 134A (green). **b**, Sensor-based detection. The sample is applied to the PNA probe-modified microsensor, and only the target mutant nucleic acids hybridize to an immobilized PNA probe. The other six mutants and wild-type nucleic acids are prevented from binding, and eventually are washed away. **c**, Electrochemical readout. After target hybridization and washing, sensors are interrogated using an electrocatalytic reporter system (left). Differential pulse voltammetry (right) is used to monitor whether a signal increase is observed in the presence of cfNA. **d**, Chip layout. Schematic of a microfabricated chip that possesses sensors that are electroplated into apertures patterned at the end of gold leads. **e**, Scanning electron microscopy image of a NME sensor.

Results and discussion

Design of the electrochemical clamp assay. The design of the electrochemical clamp assay for the detection of cfNA mutations is depicted in Fig. 1. The first detection target was the *KRAS* gene, which has seven mutations at codons 12 and 13 of two exons, which are 135A, 135C, 135T, 134A, 134C, 134T and 138A. Mutated *KRAS* (Kirsten rat sarcoma-2 virus) genes are associated with lung cancer, colorectal cancer and ovarian cancer[3,5,8,33,34], and the efficacies of several therapies are affected by mutations in this gene. A given patient sample may contain one of the seven mutant alleles and a large amount of wild-type nucleic acids (Fig. 1a). To limit the binding of all the sequences except the exact one of interest, clamps were designed to target each of the mutants and wild-type nucleic acids.

We illustrate the approach with the case of detecting the presence of a sequence that contains the 134A mutation. A mixture of six clamps that correspond to the six other *KRAS* mutations plus a single clamp that binds the wild-type sequence was added to the target-containing solution. The clamps hybridized to the six non-target mutants and the wild-type sequence, leaving the target mutant of interest unhybridized. We then introduced this solution mixture onto a sensor chip that had been functionalized with a probe corresponding to 134A. Only the mutant 134A hybridized to the probe; all the other mutants, including the wild type, were blocked by their clamps and simply remained in solution and were washed away (Fig. 1b). After 15 minutes, we read out the electrochemical signal and thereby determined the identity of the sequence.

Fabrication of the electrochemical clamp assay chip. Using photolithographic patterning, we defined an array of 40 sensors to form a bioelectronic integrated circuit (IC) (Fig. 1). Beginning with a SiO_2-coated silicon wafer, we formed contact pads and electrical leads, after which we deposited a layer of Si_3N_4 to passivate the top surface of the IC. To provide a template for the growth of the electrodeposited sensors, photolithography was used to open 5 µm apertures in the top passivation layer. We carried out Au electrodeposition at locations determined by the opened apertures to grow three-dimensional (3D) microstructures for subsequent biosensing. The microstructured sensors protruded from the surface and reached into the solution[16,21,35,36], with their size and morphology programmed by the deposition time, applied potential, Au concentration, supporting electrolyte and overcoating protocol. Nanostructures increase the sensitivity of the assay significantly[22,37–40], so we coated the Au structures with a thin layer of Pd to form finely nanostructured microelectrodes (NMEs) (Fig. 1e). The micron-size scale of the 3D electrodes increased the cross-section for the interaction with analyte molecules, whereas the nanostructure maximized the sensitivity by enhancing hybridization efficiency between the tethered probe and the analyte in solution[41].

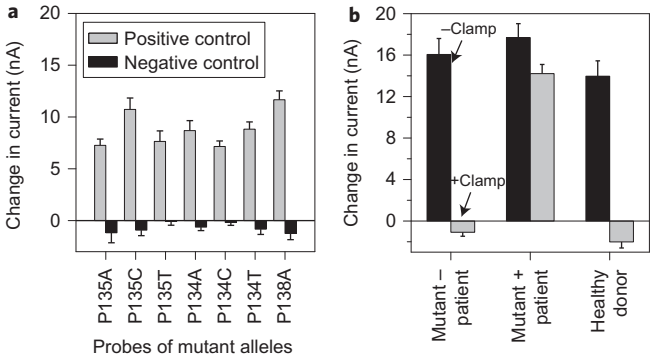

Figure 2 | Proof of principle and validation of the probes. a, Validation of seven probes (P135A, P135C, P135T, P134A, P134C, P134T and P138A) of seven mutant alleles of *KRAS*. Sensors were challenged with mixtures of nucleic acids with (positive control) and without (negative control) the mutant target of interest. The positive control contains all seven mutant oligonucleotides with 1 nM concentration of each, 100 nM of wild-type synthetic oligonucleotides, 50 pg μl^{-1} nucleic acids from healthy donors and seven clamps except the one that is complementary for the target of interest. The negative control contains all of these except the target of interest and its clamp. **b**, Current change for wild-type nucleic acids in the presence and absence of clamps at a mutant probe-modified sensor. A sensor modified with a probe specific for a mutated sequence was challenged with a mutant-negative patient sample (mutant –) in the presence (grey) and absence (black) of the clamp for the wild type, a mutant-positive patient sample (mutant +) in the presence and absence of the clamp for the wild type and a sample from the healthy donor in the presence and absence of the clamp for the wild type. Error bars represent the standard error and data represent ≥5 trials.

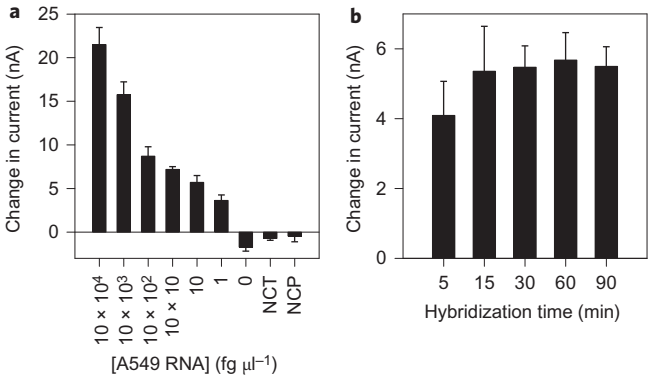

Figure 3 | Limit-of-detection studies and time dependence for *KRAS* cfNAs. a, Concentration-dependent signal change for A549 exosomal RNAs that contain all the clamps except that for 134A at the 134A mutant sensor. NCT represents the negative target, that is U373v3 exosomal RNA was used instead of A549 exosomal RNA, and NCP represents the non-complementary probe, that is A549 exosomal RNA was tested with the 135A sensor. The sensor was able to detect 1 fg μl^{-1} A549 exosomal RNA. **b**, Hybridization time-dependent signal change for the challenge of 10 fg μl^{-1} A549 exosomal RNA. After 15 minutes, 10 fg μl^{-1} A549 exosomal RNA was detectable. Error bars represent the standard error and data represent ≥5 trials.

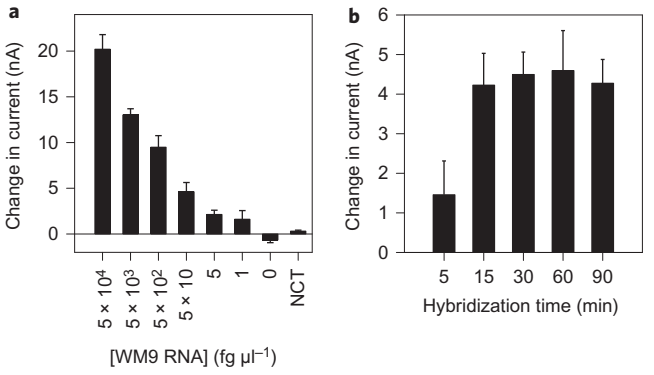

Figure 4 | Limit-of-detection studies and time dependence for *BRAF* cfNAs. The minimal amount of RNA and time needed to generate a detectable signal was determined. **a**, Concentration-dependent signal change for WM9 exosomal RNA that contained the clamp for the wild type. This analysis indicates that as little as 1 fg μl^{-1} RNA can be detected. **b**, Time-dependent signal change obtained when sensors were challenged with 50 fg μl^{-1} WM9 exosomal RNA. In as few as five minutes, a detectable signal was generated. Error bars represent the standard error and data represent ≥5 trials.

We functionalized the NMEs with PNA probes specific to the mutant target of interest (Fig. 1). After target binding and washing, we used an electrocatalytic reporter pair that comprised $Ru(NH_3)_6^{3+}$ and $Fe(CN)_6^{3-}$ to read out the presence of specific nucleic acid sequences[42]. $Ru(NH_3)_6^{3+}$ is electrostatically attracted to the negatively charged phosphate backbone of nucleic acids that binds to the probes immobilized on the surface of electrodes and is reduced to $Ru(NH_3)_6^{2+}$ when the electrode is biased at the reduction potential. The $Fe(CN)_6^{3-}$ present in solution chemically oxidized $Ru(NH_3)_6^{2+}$ back to $Ru(NH_3)_6^{3+}$, which allowed for multiple turnovers of $Ru(NH_3)_6^{3+}$ and generated a high electrocatalytic current. The difference between the pre-hybridization and the post-hybridization currents was used as a metric to determine target binding (typical differential pulse voltammograms (DPVs) before and after 100 fg μl^{-1} target mutant (134A) binding are shown in Fig. 1c).

Specific mutant detection with the clamp chip. The chip was designed to genotype seven distinct point-mutation alleles of the *KRAS* gene that are associated with lung cancer. A set of PNA probes and clamps was designed, tested and validated for sensitivity and specificity using both electrochemical (Fig. 2a) and PCR-based methods (Supplementary Fig. 1). A sample containing a complex mixture that included the complementary mutant target, non-complementary mutants, the wild-type sequence, total human RNA and the clamp cocktail was used to measure the positive signal at sensors functionalized with probes that corresponded to each mutant. A mixture that was identical, except that it lacked the complementary mutant, was tested as a negative control. The negative controls did not produce a positive signal change in any of the sensors tested; in contrast, the positive samples produced current changes that ranged from 7 to 12 nA (Fig. 2a), well above background. These results clearly demonstrate that the clamp assay can specifically detect each of the mutant alleles of *KRAS* genes. If a complementary sequence is not included in a sample, a slightly negative change in the electrochemical signal is often observed. This is a systematic effect that arises because a small amount of the probe monolayer dissociates from the sensor during incubation, which lessens the background signal.

To investigate whether the clamps were necessary for an accurate point-mutation detection, we challenged a mutant sensor with purified nucleic acids from a wild-type patient sample, a mutant-positive patient sample and a healthy donor sample in the presence and absence of the clamp for the wild-type sequence. Although hybridization and washing were performed at an elevated temperature, we observed a signal increase for all three samples if the clamp for the wild-type sequence was not present in the solution (Fig. 2b).

Table 1 | Analysis of samples from lung cancer patients.

Samples	Purified nucleic acids					Serum	
	Clamp chip*		Clamp PCR†			Clamp chip‡	
	Δ*I* (nA)	Assessment	ΔCt-1	ΔCt-2	Assessment	Δ*I* (nA)	Assessment
1	–2.3 ± 1.0	Wild type	1	16	Wild type	0 ± 0.1	Wild type
2	–1.5 ± 0.5	Wild type	–1	18	Wild type	–0.1 ± 0.1	Wild type
3	**8.3 ± 1.3**	***KRAS* mutated**	**6**	**8**	***KRAS* mutated**	**2.1 ± 0.9**	***KRAS* mutated**
4	–0.6 ± 0.7	Wild type	0	16	Wild type	–0.1 ± 0.1	Wild type
5	–1.9 ± 0.5	Wild type	–2	16	Wild type	–0.4 ± 0.2	Wild type
6	–2.5 ± 0.9	Wild type	1	14	Wild type	–0.1 ± 0.1	Wild type
7	–1.3 ± 0.6	Wild type	–4	14	Wild type	–0.4 ± 0.1	Wild type
8	–1.2 ± 0.5	Wild type	–4	18	Wild type	–0.8 ± 0.2	Wild type
9	**4.8 ± 0.7**	***KRAS* mutated**	**4**	**6**	***KRAS* mutated**	**1.3 ± 0.2**	***KRAS* mutated**
10	–1.5 ± 0.2	Wild type	–3	18	Wild type	–0.8 ± 0.2	Wild type
11	–0.6 ± 0.4	Wild type	–	-	Wild type	–0.1 ± 0.2	Wild type
12	**4.5 ± 1.4**	***KRAS* mutated**	**3**	**11**	***KRAS* mutated**	**1.4 ± 0.3**	***KRAS* mutated**
13	–2.2 ± 0.5	Wild type	–2	16	Wild type	–1.2 ± 0.1	Wild type
14	–1.5 ± 0.3	Wild type	–2	15	Wild type	0.4 ± 0.1	Wild type
HD	–1.0 ± 0.3	Wild type	0	16	Wild type	–0.5 ± 0.1	Wild type

*The sensor was challenged with total cfNAs isolated from lung cancer patients by using a commercially available kit. The threshold for this sensor was 1.25 nA. †Wild-type *KRAS* clamp PCR with total cfNAs. For the clamp PCR, ΔCt-1 ≥ 2 was considered to be mutated and ΔCt-1 < 0 was considered to be non-mutated. If 0 < ΔCt-1 < 2, another parameter, ΔCt-2, needed to be considered, and then ΔCt-2 > 6 was considered to be non-mutated. ‡The sensor was challenged with undiluted serum from a lung cancer patient. The threshold for this sensor was 0.42 nA. We used the mean + 3s.d. of healthy samples as a threshold value for the electrochemical clamp assay. If the current change for any sample was higher than the threshold, the samples was considered as *KRAS* mutated. The error values represent standard error. The cycle number at which a signal is detected above background fluorescence is termed the cycle threshold (Ct). The ΔCt-1 values are calculated by subtracting the sample Ct values from the standard Ct values, that is, ΔCt-1 = (Standard Ct) – (Sample Ct) and ΔCt-2 values are calculated by subtracting Ct values of the non PNA mix from Ct values of the samples, that is, ΔCt-2 = (Sample Ct) – (non PNA mix Ct).

Table 2 | Analysis of samples from melanoma cancer patients.

Samples	Purified nucleic acids				Serum	
	Clamp chip*		Clamp PCR†		Clamp chip‡	
	Δ*I* (nA)	Assessment	ΔCt-1	Assessment	Δ*I* (nA)	Assessment
1	5.3 ± 0.5	*BRAF* mutated	4.9	*BRAF* mutated	1.7 ± 0.3	*BRAF* mutated
2	7.9 ± 0.8	*BRAF* mutated	5.3	*BRAF* mutated	1.2 ± 0.6	*BRAF* mutated
3	0.8 ± 0.3	Wild type	–1.4	Wild type	–0.5 ± 0.1	Wild type
4	0.6 ± 0.8	Wild type	–3.1	Wild type	0.3 ± 0.4	Wild type
5	1.2 ± 0.7	Wild type	–2.1	Wild type	–1.4 ± 0.2	Wild type
6	–1.1 ± 1.0	Wild type	–1	Wild type	–0.1 ± 0.2	Wild type
7	21.9 ± 1.5	*BRAF* mutated	2	*BRAF* mutated	2.1 ± 0.3	*BRAF* mutated
HD	0.05 ± 0.6	Wild type	–1.2	Wild type	0.3 ± 0.1	Wild type

*The sensor was challenged with total cfNAs isolated from melanoma patients by using a commercially available kit. The threshold for this sensor was 2.46 nA. †Wild-type *BRAF* clamp PCR with total cfNAs. For the clamp PCR, according to the manufacturer, ΔCt-1 ≥ 2 was considered to be mutated and ΔCt-1 < 0 was considered to be non-mutated. ‡The sensor was challenged with undiluted melanoma patient serum. The threshold for this sensor was 0.69 nA. We used the mean + 3s.d. of healthy samples as a threshold value for the electrochemical clamp assay. If the current change for any sample was higher than the threshold, the sample was considered as *BRAF* mutated. The error values represent standard error.

However, in the presence of the clamp for the wild-type sequence, we did not observe any positive signal change for the mutant-negative and healthy donor samples. A significant signal change was observed for the mutant-positive sample in the presence of the clamp. The change of current in the presence of the clamp was slightly lower than that in the absence of the clamp because the clamp minimizes interference from wild-type nucleic acids. These results clearly show that for the sensitive and specific detection of mutations within cfNAs, the presence of the clamp sequence is essential.

To evaluate the sensitivity of our clamp assay, we investigated the dependence of the electrochemical signal on concentration when the sensors were challenged with RNA isolated from A549 cells that carried the 134A mutation. RNA that contained the wild-type sequence was isolated from U373v3 cells and used to evaluate the specificity. To identify the detection limit of our assay, we tested concentrations of RNA ranging from 1 fg μl^{-1} to 100 pg μl^{-1} (Fig. 3a). The signal change increased with increasing concentration of the target over six orders of magnitude. Moreover, to observe the specificity of the sensor further we performed three additional control experiments: testing of a blank and a non-complementary RNA target (NCT of Fig. 3a), and using a non-complementary probe. For all three controls, we obtained a limit of detection of 1 fg μl^{-1}. To evaluate the detection speed of the clamp assay, we investigated the time-dependent signal change by varying the hybridization time of the 10 fg μl^{-1} target RNA (Fig. 3b). The electrochemical clamp assay is capable of delivering results very rapidly: statistically significant signals were obtained within five minutes.

To establish that the clamp method is generally applicable to other sequences, we investigated the detection of mutations within *BRAF*, which are associated with melanoma, the deadliest form of skin cancer[6]. After we had validated a set of BRAF-specific probes, we checked the specificity and sensitivity of the clamp assay for RNA from the WM9 cell line (Fig. 4a,b). In this case, we also obtained a similar sensitivity, specificity and speed of the clamp assay.

Patient-sample analysis. The ultimate goal of our effort to develop a mutation-discriminating chip was to enable the direct analysis of mutated sequences in patient samples. We challenged our electrochemical clamp assay with the task of analysing cfNA in serum samples from lung cancer patients (*KRAS*) and melanoma cancer patients (*BRAF*) (Tables 1 and 2). In the trials analysing samples for *KRAS* mutations, a universal probe mixture (Supplementary Fig. 2 and Supplementary Table 3) was used that

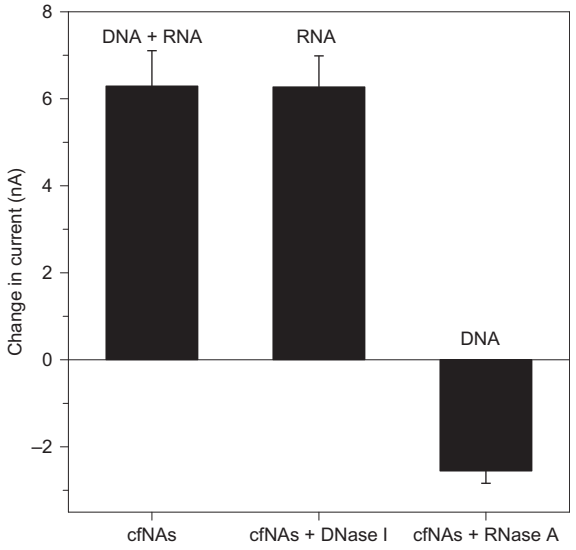

Figure 5 | Determination of target analyte. Both cfRNA and cfDNA have been found in patient samples, and the sensing approach described cannot directly discriminate which type of nucleic acid is present. By introducing enzymes that can digest either RNA or DNA specifically, the type of cfNA can be determined. Three different samples were tested: Left, cfNAs only. Centre, DNase I digested cfNAs. Right, RNase A digested cfNAs. The loss of signal for RNase A digested cfNAs. Indicates that RNA is the material being detected in the assay described. Error bars represent the standard error and data represent ≥5 trials.

allowed us to screen for all of the possible types of mutations in cfNAs using a single experiment. This approach leverages a mixture of sequences that are perfect complements to all the known mutants of the sequences of interest. By using this universal probe approach, it is possible to use a single reaction to look for all the possible mutations.

cfNAs were isolated and purified from serum, using commercially available kits, from 14 lung cancer and nine melanoma patients. Serum from a healthy donor was also processed in the same way and analysed. Three of the samples from the 14 lung cancer patients were positive for *KRAS* mutations and four of the samples from the nine melanoma cancer patients were positive for *BRAF* mutations. For each sample analysed using the electrochemical method, the mean signal plus three times the standard deviation (mean + 3s.d.) for a sample from a healthy donor was used as a cutoff value. If the current level observed with a patient sample was higher than the cutoff value, the sample was determined to be positive for the mutation, and if it was lower, the sample was negative for the mutation. In each case, a previously validated clamp PCR[43,44] method was used to confirm the presence or absence of the *KRAS* and *BRAF* mutations, and the results were in agreement with the electrochemical clamp assay results.

We also challenged the clamp assay with undiluted serum from the same lung cancer and melanoma patients (Tables 1 and 2). The signal changes observed in the undiluted serum were lower than those for purified samples, which is expected because the concentrations of the cfNAs were much lower than those in the purified samples. Nonetheless, the mutated cfNAs were identified correctly in each of the patient samples.

The clamp assay thus successfully detects cfNA *KRAS* and *BRAF* mutations directly in the undiluted serum of lung cancer and melanoma patients. However, the clamp PCR was not able to detect *KRAS* and *BRAF* directly in undiluted patient serum. We investigated the PCR-based method with undiluted serum, but did not observe any detectable levels of enzymatic amplification (Supplementary Fig. 3). We also explored the application of literature protocols[45] that have been used successfully to amplify viral targets in unpurified serum. We diluted the same patient serum fivefold in PBS and tested these samples along with those that had undergone heat treatment. The PCR amplification of mutated sequences was not successful, despite the application of these protocols (Supplementary Fig. 3). The fact that this treatment of serum was successful for the viral targets versus the cfNAs studied here probably relates to the very low levels of the mutated sequences under analysis here relative to the higher abundances of viral sequences. This set of studies clearly indicates that, although the chip-based clamp assay can be applied successfully to unpurified serum samples, PCR is not amenable to the same type of direct sample analysis. The direct analysis of patient samples, without the requirement of purification, is a significant advantage, as it eliminates any issues related to bias in the pool of sequences that are isolated. In addition, very small volumes (50 µl) of serum can be analysed with this approach, whereas 5 ml of serum is required to yield enough purified cfNA for analysis via PCR.

Although the experiments described above established the sensitivity and specificity of cfNA analysis with the electrochemical clamp assay, they did not, on their own, distinguish between DNA or RNA analytes. To identify whether the assay was interrogating genomic DNA or transcribed mRNA, we challenged our clamp assay with cfNAs, cfNAs digested with DNase I and cfNAs digested with RNase A. The changes for total cfNAs and cell-free RNAs (cfRNAs) were similar, whereas no signal change was observed for cell-free DNA (cfDNA) (Fig. 5). We conclude that the analytes detected were predominantly cfRNAs[4]. Indeed, the assay relies on no steps to denature or fragment the cfNAs, and the sensitivity to RNA is therefore to be expected.

Conclusion

We analysed the cfNAs (both cfDNA and cfRNA) of lung cancer and melanoma patients using a highly specific and sensitive electrochemical clamp assay. The clamp chip accurately detected mutated sequences of cfNA directly in the patient serum. The clamp assay requires a collection of sequences that effectively compete with the sequence of interest and only allows the specific target to bind to the chip. The minimally invasive serum analyses of cfNA offer a simpler alternative to cancer-tissue biopsies. They also suggest a means to monitor drug responses and treatment effectiveness. Furthermore, the chip-based approach we describe has a number of advantages over existing methods that have been used to analyse cfNAs. The clamp assay produces the same accuracy as PCR, but it is functional when unpurified serum is used as the sample type. This leads to a much simpler assay workflow, minimizes sample loss and permits the analysis of small samples. The sensitivity of the clamp assay chip is extremely high, and allows for the use of samples that can be collected non-invasively to profile the mutational spectrum of a tumour. The analysis time required, which can be as short as five minutes, is significantly more rapid than the 2–3 hours required for PCR, and the days required for sequencing. Finally, the use of a chip-based format for the assay will allow a straightforward automation of the approach and a low cost per test.

Materials and methods

Nucleic acids. All of the PNA probes and PNA clamps were obtained from PNA Bio. PCR primers and synthetic DNA targets were obtained from ACGT (see the Supplementary Information for more details).

Fabrication of NMEs. Fabrication of the chips and growth of the NMEs were performed as described previously[37]. The control of the sensor surface area has been characterized extensively[46], and in this study the average surface area was $4.75 \pm 0.3 \times 10^{-4}$ cm^2 as determined by electrochemical Pd oxide stripping.

Clamp chip protocol. A 2 µM probe solution in water was prepared from a 20% acetonitrile solution containing a 100 µM PNA probe. The probe solution was then

heated to 65 °C for five minutes and chilled on ice for five minutes before deposition. The solution (50 µl) was dropped onto the chips and incubated overnight in a dark humidity chamber at room temperature to immobilize the probe. The effect of the deposition conditions on the probe surface coverage has been studied extensively[38], and the conditions used here led to a surface coverage of 2×10^{13} molecules cm^{-2}. The chip was then washed for ten minutes with PBS at 60 °C followed by washing for ten minutes at room temperature. After the initial electrochemical scanning, the chips were treated with different targets at 60 °C. The optimal hybridization time was determined to be 15 minutes. After washing for ten minutes with PBS at 55 °C followed by washing for ten minutes at room temperature, the final electrochemical scan of the chip was performed.

cfNA isolation from exosomes. WM9 and U373v3 exosomes were isolated by an ultracentrifugation method and RNA was extracted by Trizol (Invitrogen). A549 exosomal RNA (mutant *KRAS* 134A) and exosomal RNA from patient sera were extracted using Norgen Biotek kit catalogue number 51000. The isolated RNA had an A260/A280 ratio >2, which indicates a high level of purity.

cDNA synthesis and clamp PCR. A volume of 2 µl purified cfNA (30–754 ng) was used for the cDNA synthesis in a 20 µl reaction mixture with random hexamer primers and Superscript III reverse transcriptase (Invitrogen kit). A volume of 2 µl cDNA was used in a 50 µl non-competitive clamp PCR reaction with a 2 µM final concentration of gene-specific primers, or in a 20 µl real-time clamp PCR reaction mixture (Panagene kit).

Mutant *BRAF* and mutant *KRAS* clamp optimizations. To validate that 60 °C was an appropriate specific temperature for the sensor assay, clamp PNA was tested in a qualitative PCR assay. The PCR programme was as follows: template denaturing at 95 °C for three minutes followed by 35 cycles of template denaturing at 95 °C for 30 seconds, primer annealing and DNA chain extension at 60 °C for one minute. The PCR products were visualized using agarose gel electrophoresis.

Real-time competitive clamp PCR. Mutant *BRAF* and mutant *KRAS* real-time competitive clamp PCRs were performed using a Panagene kit (mutant *BRAF* product number PNAC-2001 and mutant *KRAS* product number PNAC-1002). The real-time clamp PCR was performed on an ABI 7500 thermocycler and the SYBR Green reading was set at 72 °C. The PCR programme was as follows: template denaturing at 94 °C for five minutes followed by 40 cycles of template denaturing at 94 °C for 30 seconds, PNA clamp at 70 °C for 20 seconds, primer annealing at 63 °C for 30 seconds and DNA chain extension at 72 °C for 30 seconds.

***KRAS* and *BRAF* detection in whole serum.** For mutation detection in whole serum we co-deposited 6-mercaptohexanol (MCH) with the probe to minimize nonspecific binding. For the *KRAS* mutation detection, we used a universal probe for *KRAS* point mutations that was a combination of all of the possible mutant probes. An aqueous solution that contained 2 µM PNA probes was heated to 65 °C for five minutes and, after chilling on ice for five minutes, 18 µM MCH was mixed with this probe solution. After that the solution was dropped onto a chip, kept overnight and then washed as described above. The serum sample was prepared by adding 12.5 µl of lysis buffer (1 × PBS containing 10% NP40 and 10% Triton X100), 1 µl of 10 µM clamps for the wild type and 3 µl of RNase inhibitor (Ambion, Am 2694) to 50 µl of that patient's serum. After the initial electrochemical scanning described above, the serum sample was dropped onto a chip and incubated at 60 °C for 15 minutes. After washing, a final electrochemical scan was performed.

Electrochemical analysis. Signal changes that correspond to specific targets were calculated with background-subtracted currents: change in currents = $(I_{after} - I_{before})$, where I_{after} = current after target binding and I_{before} = current before target binding (see the Supplementary Information for details).

Received 15 October 2014; accepted 21 April 2015; published online 1 June 2015

References

1. Stroun, M., Anker, P., Lyautey, J., Lederrey, C. & Maurice, P. A. Isolation and characterization of DNA from the plasma of cancer-patients. *Eur. J. Cancer Clin. Oncol.* **23,** 707–712 (1987).
2. Kaiser, J. Keeping tabs on tumor DNA. *Science* **327,** 1074 (2010).
3. Newman, A. M. *et al.* An ultrasensitive method for quantitating circulating tumor DNA with broad patient coverage. *Nature Med.* **20,** 548–556 (2014).
4. Schwarzenbach, H., Hoon, D. S. B. & Pantel, K. Cell-free nucleic acids as biomarkers in cancer patients. *Nature Rev. Cancer* **11,** 426–437 (2011).
5. Thierry, A. R. *et al.* Clinical validation of the detection of *KRAS* and *BRAF* mutations from circulating tumor DNA. *Nature Med.* **20,** 430–436 (2014).
6. Huber, F., Lang, H. P., Backmann, N., Rimoldi, D. & Gerber, C. Direct detection of a *BRAF* mutation in total RNA from melanoma cells using cantilever arrays. *Nature Nanotechnol.* **8,** 125–129 (2013).
7. Diehl, F. *et al.* Circulating mutant DNA to assess tumor dynamics. *Nature Med.* **14,** 985–990 (2008).
8. Bettegowda, C. *et al.* Detection of circulating tumor DNA in early- and late-stage human malignancies. *Sci. Transl. Med.* **6,** 224ra24 (2014).
9. Murtaza, M. *et al.* Non-invasive analysis of acquired resistance to cancer therapy by sequencing of plasma DNA. *Nature* **497,** 108–113 (2013).
10. Ørum, H. *et al.* Single base pair mutation analysis by PNA directed PCR clamping. *Nucleic Acids Res.* **21,** 5332–5336 (1993).
11. Taback, A. *et al.* Peptide nucleic acid clamp PCR: a novel K-ras mutation detection assay for colorectal cancer micrometastases in lymph nodes. *Int. J. Cancer* **111,** 409–414 (2004).
12. Chiou, C-C., Luo, J-D. & Chen, T-L. Single-tube reaction using peptide nucleic acid as both PCR clamp and sensor probe for the detection of rare mutations. *Nature Protocols* **1,** 2604–2612 (2007).
13. García-Olmo, D. C. *et al.* Colorectal cancer patients induce the oncogenic transformation of susceptible cultured cells. *Cancer Res.* **70,** 560–567 (2010).
14. Kelley, S. O. *et al.* Advancing the speed, sensitivity and accuracy of biomolecular detection using multi-length-scale engineering. *Nature Nanotechnol.* **9,** 969–980 (2014).
15. Bakker, E. & Qin, Y. Electrochemical sensors. *Anal. Chem.* **78,** 3965–3983 (2006).
16. Das, J. & Kelley, S. O. Protein detection using arrayed microsensor chips: tuning sensor footprint to achieve ultrasensitive readout of CA-125 in serum and whole blood. *Anal. Chem.* **83,** 1167–1172 (2011).
17. Wen, Y. *et al.* DNA nanostructure-based interfacial engineering for PCR-free ultrasensitive electrochemical analysis of microRNA. *Sci. Rep.* **2,** 867 (2012).
18. Chuah, K. *et al.* Ultrasensitive electrochemical detection of prostate-specific antigen (PSA) using gold-coated magnetic nanoparticles as 'dispersible electrodes'. *Chem. Commun.* **48,** 3503–3505 (2012).
19. Si, Y. *et al.* Ultrasensitive electroanalysis of low-level free microRNAs in blood by maximum signal amplification of catalytic silver deposition using alkaline phosphatase-incorporated gold nanoclusters. *Anal. Chem.* **86,** 10406–10414 (2014).
20. Rusling, J. F. Multiplexed electrochemical protein detection and translation to personalized cancer diagnostics. *Anal. Chem.* **85,** 5304–5310 (2013).
21. Fang, Z. *et al.* Direct profiling of cancer biomarkers in tumour tissue using a multiplexed nanostructured microelectrode integrated circuit. *ACS Nano* **3,** 3207–3213 (2009).
22. Soleymani, L. *et al.* Hierarchical nanotextured microelectrodes overcome the molecular transport barrier to achieve rapid, direct bacterial detection. *ACS Nano* **5,** 3360–3366 (2011).
23. Ferguson, B. S. *et al.* Genetic analysis of H1N1 influenza virus from throat swab samples in a microfluidic system for point-of-care diagnostics. *J. Am. Chem. Soc.* **133,** 9129–9135 (2011).
24. Hsieh, K., Patterson, A. S., Ferguson, B. S., Plaxco, K. W. & Soh, H. T. Rapid, sensitive, and quantitative detection of pathogenic DNA at the point of care through microfluidic electrochemical quantitative loop-mediated isothermal amplification. *Angew. Chem. Int. Ed.* **51,** 4896–4900 (2012).
25. Yang, H. *et al.* Direct, electronic microRNA detection for the rapid determination of differential expression profiles. *Angew. Chem. Int. Ed.* **48,** 8461–8464 (2009).
26. Wu, Y. & Lai, R. Y. Development of a 'signal-on' electrochemical DNA sensor with an oligo-thymine spacer for point mutation detection. *Chem. Commun.* **49,** 3422–3424 (2013).
27. Wee, E. J. H., Shiddiky, M. J. A., Brown, M. A. & Trau, M. ELCR: electrochemical detection of single DNA base changes via ligase chain reaction. *Chem. Commun.* **48,** 12014–12016 (2012).
28. Xiang, Y. & Lu, Y. Using personal glucose meters and functional DNA sensors to quantify a variety of analytical targets. *Nature Chem.* **3,** 697–703 (2011).
29. Drummond, T. G., Hill, M. G. & Barton, J. K. Electrochemical DNA sensors. *Nature Biotechnol.* **21,** 1192–1199 (2003).
30. Ge, Z. *et al.* Hybridization chain reaction amplification of microRNA detection with a tetrahedral DNA nanostructure-based electrochemical biosensor. *Anal. Chem.* **86,** 2124–2130 (2014).
31. Hsieh, K., Patterson, A. S., Ferguson, B. S., Plaxco, K. W. & Soh, H. T. Rapid, sensitive, and quantitative detection of pathogenic DNA at the point of care via microfluidic electrochemical quantitative loop-mediated isothermal amplification (MEQ-LAMP). *Angew. Chem. Int. Ed.* **124,** 4980–4984 (2012).
32. Tavallaie, R., Darwish, N., Gebala, M., Hibbert, D. B. & Gooding, J. J. The effect of interfacial design on the electrochemical detection of DNA and microRNA using methylene blue at low-density DNA films. *ChemElectroChem* **1,** 165–171 (2014).
33. Gautschi, O. *et al.* Origin and prognostic value of circulating *KRAS* mutations in lung cancer patients. *Cancer Lett.* **254,** 265–273 (2007).
34. Wang, S. *et al.* Potential clinical significance of a plasma-based *KRAS* mutation analysis in patients with advanced non-small cell lung cancer. *Clin. Cancer Res.* **16,** 1324–1330 (2010).
35. Soleymani, L., Fang, Z., Sargent, E. H. & Kelley, S. O. Programming the detection limits of biosensors through controlled nanostructuring. *Nature Nanotechnol.* **4,** 844–848 (2009).
36. Soleymani, L. *et al.* Nanostructuring of patterned microelectrodes to enhance the sensitivity of electrochemical nucleic acids detection. *Angew. Chem. Int. Ed.* **48,** 8457–8460 (2009).
37. Das, J. *et al.* An ultrasensitive universal detector based on neutralizer displacement. *Nature Chem.* **4,** 642–648 (2012).

38. Das, J. & Kelley, S. O. Tuning the bacterial detection sensitivity of nanostructured microelectrodes. *Anal. Chem.* **85,** 7333–7338 (2013).
39. Lam, B. *et al.* Solution-based circuits enable rapid and multiplexed pathogen detection. *Nature Commun.* **4,** 2001 (2013).
40. Besant, J. D., Das, J., Sargent, E. H. & Kelley, S. O. Proximal bacterial lysis and detection in nanoliter wells using electrochemistry. *ACS Nano* **7,** 8183–8189 (2013).
41. Bin, X., Sargent, E. H. & Kelley, S. O. Nanostructuring of sensors determines the efficiency of biomolecular capture. *Anal. Chem.* **82,** 5928–5931 (2010).
42. Lapierre, M. A., O'Keefe, M. M., Taft, B. J. & Kelley, S. O. Electrocatalytic detection of pathogenic DNA sequences and antibiotic resistance markers. *Anal. Chem.* **75,** 6327–6333 (2003).
43. *PNAClamp KRAS Mutation Detection Kit (Ver.2), Instruction Manual for Product #PNAC-1002* Version 4.1 (PNAGENE, 2012).
44. *PNAClamp BRAF Mutation Detection Kit, Instruction Manual for Product #PNAC-2001* Version 4.4 (PNAGENE, 2012).
45. Abe, K. Direct PCR from serum: application to viral genome detection in *PCR Protocols* (eds Bartlett, J. M. S. & Stirling, D.) 161–166 (Tatowa, 2003).
46. Zhou, Y., Wan, Y., Sage, A., Poudineh, M. & Kelley, S. O. Effect of microelectrode structure on electrocatalysis at nucleic acid-modified sensors. *Langmuir* **30,** 14322–14328 (2014).

Acknowledgements

This research was sponsored by the Ontario Research Fund (Research Excellence Award to S.O.K.), the Canadian Institutes for Health Research (Emerging Team Grant to S.O.K. and E.H.S.), the Canadian Cancer Society Research Institute (Innovation Grant No. 702414 to S.O.K. and J.R.) and the Natural Science and Engineering Research Council (Discovery Grant to S.O.K.).

Author contributions

J.D., I.I., J.R., E.H.S. and S.O.K. conceived the experiments, J.D. and I.I. designed the experiments, L.M. contributed critical materials and J.D., I.I., E.H.S. and S.O.K. co-wrote the paper. All the authors reviewed and improved the paper.

Additional information

Supplementary information is available in the online version of the paper. Reprints and permissions information is available online at www.nature.com/reprints. Correspondence and requests for materials should be addressed to S.O.K.

Competing financial interests

The authors declare no competing financial interests.